

Journal of Semiconductors

JOS

iopscience.iop.org/jos
www.jos.ac.cn

Silicon-integrated high-speed mode and polarization switch-and-selector

Yihang Dong, Yong Zhang, Jian Shen, Zihan Xu, Xihua Zou, and Yikai Su

Citation: Y H Dong, Y Zhang, J Shen, Z H Xu, X H Zou, and Y K Su, Silicon-integrated high-speed mode and polarization switch-and-selector[J]. *J. Semicond.*, 2022, 43(2).

View online: <https://doi.org/10.1088/1674-4926/43/2/022301>

Articles you may be interested in

[Design of a C-band polarization rotator-splitter based on a mode-evolution structure and an asymmetric directional coupler](#)

Journal of Semiconductors. 2018, 39(12), 124008 <https://doi.org/10.1088/1674-4926/39/12/124008>

[Emerging technologies in Si active photonics](#)

Journal of Semiconductors. 2018, 39(6), 061001 <https://doi.org/10.1088/1674-4926/39/6/061001>

[Recent progress in integrated electro-optic frequency comb generation](#)

Journal of Semiconductors. 2021, 42(4), 041301 <https://doi.org/10.1088/1674-4926/42/4/041301>

[Recent advances of heterogeneously integrated III-V laser on Si](#)

Journal of Semiconductors. 2019, 40(10), 101304 <https://doi.org/10.1088/1674-4926/40/10/101304>

[Recent progress in epitaxial growth of III-V quantum-dot lasers on silicon substrate](#)

Journal of Semiconductors. 2019, 40(10), 101302 <https://doi.org/10.1088/1674-4926/40/10/101302>

[Perspective: optically-pumped III-V quantum dot microcavity lasers via CMOS compatible patterned Si \(001\) substrates](#)

Journal of Semiconductors. 2019, 40(10), 101303 <https://doi.org/10.1088/1674-4926/40/10/101303>



关注微信公众号，获得更多资讯信息

Silicon-integrated high-speed mode and polarization switch-and-selector

Yihang Dong¹, Yong Zhang^{1, †}, Jian Shen¹, Zihan Xu¹, Xihua Zou², and Yikai Su^{1, †}

¹State Key Lab of Advanced Optical Communication Systems and Networks, Department of Electronic Engineering, Shanghai Jiao Tong University, Shanghai 200240, China

²Center for Information Photonics and Communications, School of Information Science and Technology, Southwest Jiao Tong University, Chengdu 611756, China

Abstract: On-chip optical communications are growingly aiming at multimode operation together with mode-division multiplexing to further increase the transmission capacity. Optical switches, which are capable of optical signals switching at the nodes, play a key role in optical networks. We demonstrate a 2×2 electro-optic Mach-Zehnder interferometer-based mode- and polarization-selective switch fabricated by standard complementary metal-oxide-semiconductor process. An electro optic tuner based on a PN-doped junction in one of the Mach-Zehnder interferometer arms enables dynamic switching in 11 ns. For all the channels, the overall insertion losses and inter-modal crosstalk values are below 9.03 and -15.86 dB at 1550 nm, respectively.

Key words: mode and polarization switch-and-selector; silicon photonics; high speed

Citation: Y H Dong, Y Zhang, J Shen, Z H Xu, X H Zou, and Y K Su, Silicon-integrated high-speed mode and polarization switch-and-selector[J]. *J. Semicond.*, 2022, 43(2), 022301. <http://doi.org/10.1088/1674-4926/43/2/022301>

1. Introduction

Given the ever-increasing internet traffic, scaling the per-fiber transmission capacity is highly desired^[1]. Several multiplexing schemes, including wavelength-division multiplexing (WDM), polarization-division multiplexing (PDM), and mode-division multiplexing (MDM), are exploited to increase the communication capacity. Among them, MDM provides an attractive option to further expand the transmission capacity by introducing multiple modes for each wavelength carrier^[2, 3].

Silicon optical switches based on a silicon-on-insulator platform offer the potential to enable high-speed optical networks due to their compatibility with a commercial complementary metal-oxide-semiconductor (CMOS) process^[4–6]. When leveraging multiple physical dimensions, a two-dimensional or three-dimensional switch can be realized to achieve scaled capacity. An on-chip multimode optical switch was reported based on quasi-phase-matching and a staged coupling method with the capability of three-wavelength and two-mode multiplexing^[7]. Recently, a WDM-compatible multimode optical switch working for three wavelengths and two modes was demonstrated^[8]. A silicon wavelength and mode switch-and-selector architecture with two wavelengths and two modes was reported with improved flexibility of the network^[9]. In contrast, mode and polarization dimensions own the merit of multiplexing signals with one laser source. Recently, silicon optical switches carrying four-mode and two-mode dual-polarization were demonstrated using Mach-Zehnder interferometers (MZIs), respectively^[10, 11]. To further

scale the capacity, we presented a switch with three hybrid dimensions including mode, polarization and wavelength^[12]. However, previous multi-dimensional switches were based on thermo-optic tuning with a slow response time of several μ s. Dynamic and high-speed multi-dimensional optical switching is highly desired.

In this paper, we report a 2×2 high-speed mode and polarization switch-and-selector architecture (HMPSA) based on MZI switches with PN junction-based phase shifters. Compared to thermo-optic switches, the electro-optic (EO) HMPSA exhibits a fast switching time of 11 ns benefiting from the free-carrier plasma dispersion effect. Moreover, the numbers of the MZIs are reduced by half in this configuration. The measured overall insertion losses (ILs) are below 9.03 dB. The inter-modal and intra-modal crosstalk (XT) of the HMPSA are lower than -15.86 and -7.32 dB for all the channels at 1550 nm, respectively.

2. Structure and design

The architecture of the silicon-integrated HMPSA for two modes and dual polarizations is shown in Fig. 1(a). Similarly to a wavelength switch-and-selector architecture, the HMPSA can route any optical signal from one input port to an arbitrary output port.

The proposed switches consist of mode polarization beam splitters (PBSs), mode multiplexers (MMUXs), polarization rotators (PRs) and crossings. The mode multiplexers are based on asymmetric directional couplers to multiplex the TE_1 and TM_1 modes^[13]. The crossings are implemented by 90° -crossed multi-mode interferometer (MMIs)^[14]. The polarization beam splitters and rotators are the building blocks of the process design kit (PDK) from Advanced Micro Foundry (AMF)^[15]. The device has two input ports (I_1, I_2) and two out-

Correspondence to: Y Zhang, yongzhang@sjtu.edu.cn; Y K Su, yikaisu@sjtu.edu.cn

Received 12 AUGUST 2021; Revised 12 OCTOBER 2021.

©2022 Chinese Institute of Electronics

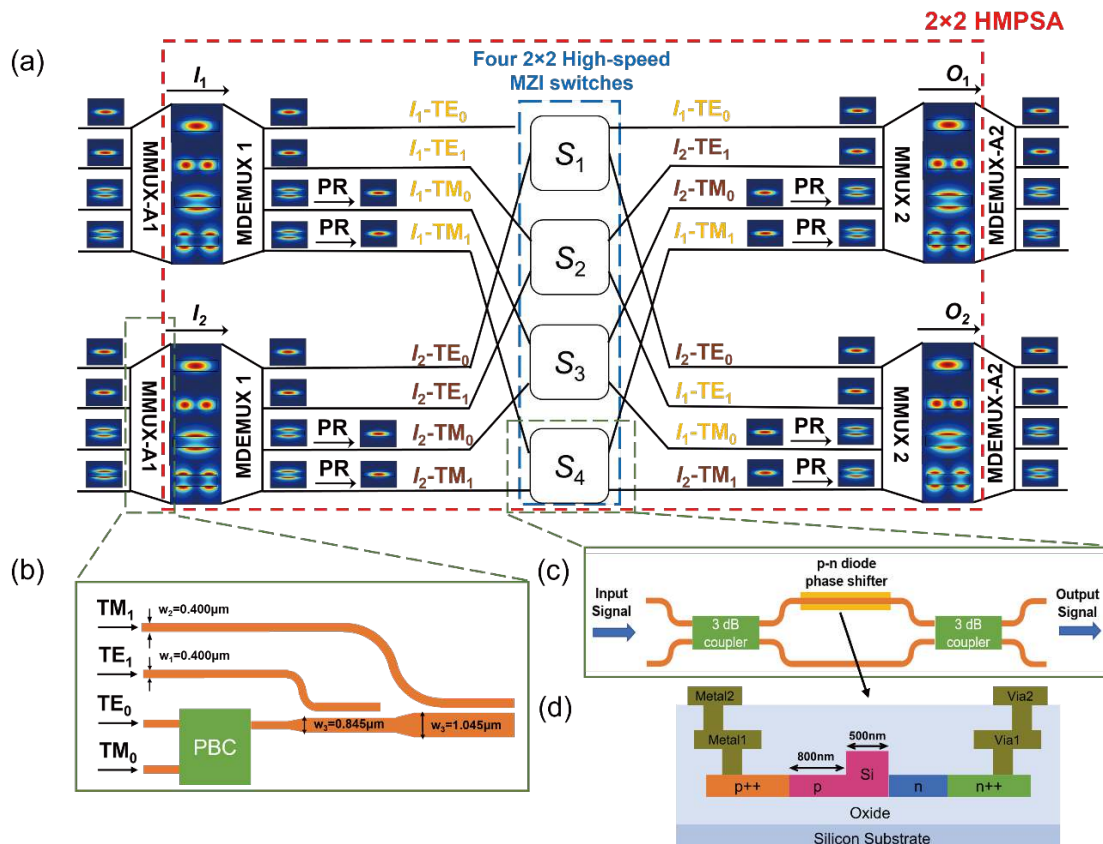


Fig. 1. (Color online) (a) Architecture of the proposed 2×2 HMPSA (The calculated mode patterns of the TE_0, TE_1, TM_0 and TM_1 modes are intensity profiles). Structures of (b) MMUX and (c) 2×2 high-speed MZI switch. (d) Cross-sectional view of the PN phase shifter. (MMUX-A: auxiliary mode multiplexer; MDEMUX-A: auxiliary mode de-multiplexer.)

put ports (O_1, O_2). Firstly, the four mode- and polarization-multiplexed channels with TE_0, TE_1, TM_0 and TM_1 modes from an input port I_1 or I_2 are converted to the fundamental modes by the corresponding mode de-multiplexers (MDEMUXs) and the PBSs. After rotating the TM fundamental mode to the TE fundamental mode by PRs, signals are switched to the output waveguides by the follow-on MZI-based EO switches. After the TM channels are recovered by the PRs, the switched signals are multiplexed by the MMUXs and the polarization beam combiners (PBCs) and finally routed to output port O_1 or O_2 .

Various structures have been used as MMUX, such as Y-splitters^[16, 17], MMI coupler^[18] and asymmetrical directional couplers^[19, 20]. Here we choose asymmetric directional couplers to achieve mode (de-)multiplexing for their better compactness in this design. As shown in Fig. 1(b), the widths of the waveguides carrying the two modes and dual polarization are chosen to be 0.4, 0.845, 0.4 and 1.045 μm , respectively. We use 10- μm -length adiabatic tapers to connect the multimode waveguides of different widths. For TE_1 and TM_1 modes, the optimized gaps between the access waveguides and the multimode waveguides are 0.2 and 0.3 μm , respectively. The coupling lengths are designed as 18.5 and 8.25 μm , respectively. The coupling between a few-mode fiber and a silicon multimode waveguide is still challenging^[21–23]. Consequently, two MMUX-As and two MDEMUX-As outside the 2×2 HMPSA are used to couple high-order modes.

Fig. 1(c) depicts the schematic configuration of the 2×2 high-speed MZI switch. A 2×2 MMI structure is used as the

3 dB coupler for its compact size and broad-band response. One arm of the MZI contains an EO phase shifter based on a lateral 50- μm -long p-n diode to induce the π phase shift for high-speed switching operations.

3. Fabrication and results

The fabrication of the HMPSA chip is carried out by ultra-violet lithography on a silicon-on-insulator wafer with a 220-nm-thick silicon layer on 2 μm buried dioxide layer using CMOS processes in AMF, Singapore. Fig. 2(a) shows the micrograph of the fabricated 2×2 HMPSA with a footprint of $2.2 \times 0.9 \text{ mm}^2$. Fig. 2(b)–2(e) depict magnified micrographs of a PBS, a MMUX, a PR, a 2×2 high-speed MZI switch and waveguide crossings, respectively.

In the experiment setup, a tunable light source (Keysight 81960A) and an optical power meter (Keysight N7744A) are utilized to measure the spectral responses of the HMPSA. Light is coupled into and out of the HMPSA by grating couplers with a shallow etching depth of 70 nm and periods of 630 and 980 nm for supporting TE and TM polarization, respectively. The fiber-to-chip coupling losses are 5.3 and 6.4 dB/facet at 1550 nm, respectively. Fig. 3 shows the measured transmission spectra, which have been normalized by the grating couplers and the MMUX on the same chip. Table 1 summarizes the ILs performance of the building blocks. Take the input port I_1 of TE_0 channel as an example. When the powers supplied to the heater are 6.23 and 29.03 mW, the signals are switched to output port O_1 and O_2 , respectively. By tuning the powers applied to the corresponding MZI switches, optic-

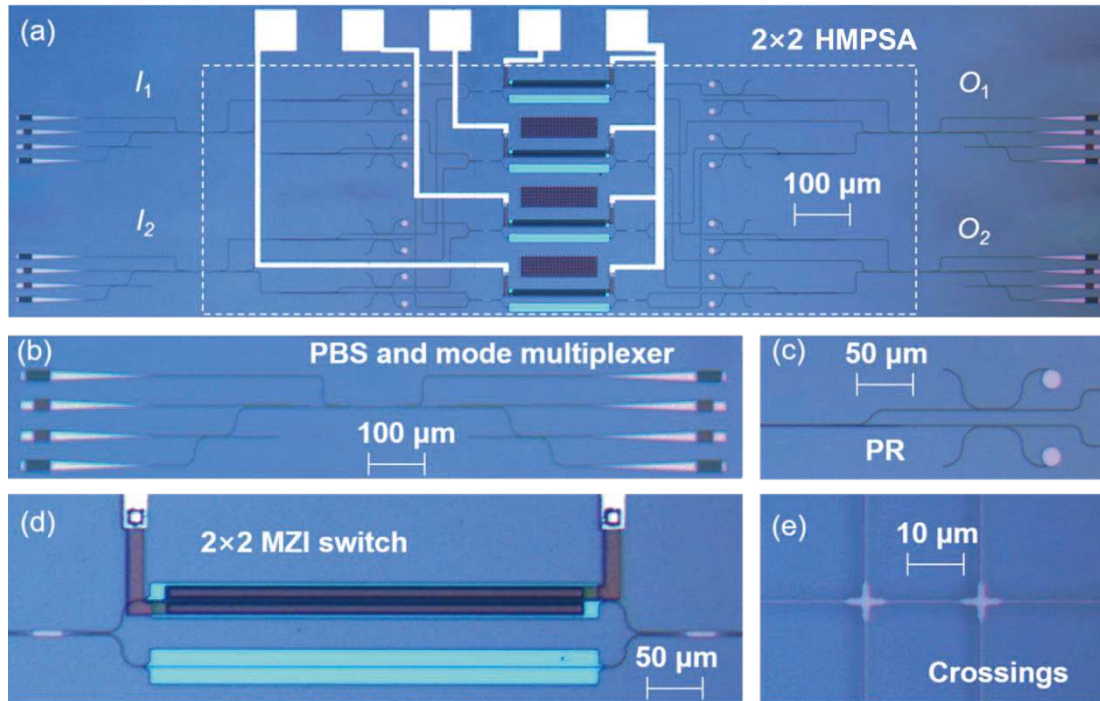


Fig. 2. (Color online) (a) Micrograph of a silicon chip including a HMPSA. Magnified micrographs of (b) a PBS and a MMUX, (c) a PR, (d) a MZI switch and (e) waveguide crossings.

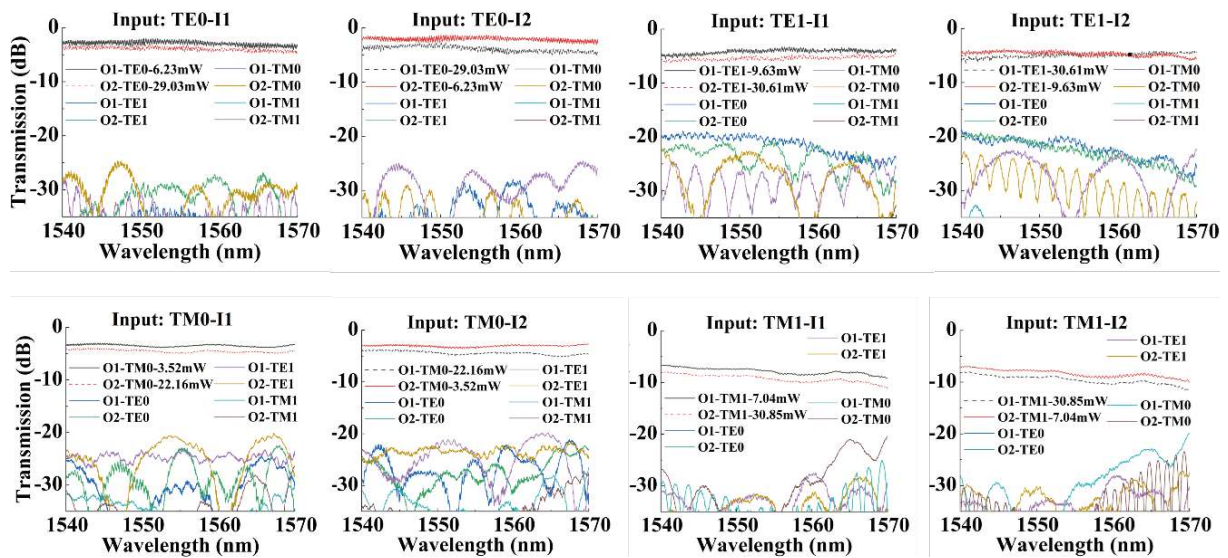


Fig. 3. (Color online) Results of measured inter-modal crosstalk.

Table 1. Measured insertion losses of the building blocks.

Item	Loss
Grating coupler for TE ₀	5.3 dB/facet
Grating coupler for TM ₀	6.4 dB/facet
PBS for TE ₀	0.98 dB
PBS for TM ₀	1.04 dB
PR for TE ₀	0.91 dB
PR for TM ₀	0.78 dB
MMUX for TE ₀	1.61 dB
MMUX for TM ₀	1.32 dB

al signal from each input port is capable of being routed to all available output ports for all the channels. Here we manually adjusted the switching power to allow the maximum out-

put optical power, while it is possible to achieve switch control and calibration with built-in power monitors and a feedback loop^[24, 25]. For all the channels, the ILs are below 9.03 dB at 1550 nm, which are mainly caused by the manufacturing imperfection, incomplete coupling in the MMUXs and the PBSs. The ILs can be reduced by using dual-core adiabatic tapers^[26] or higher silicon layer thickness^[27] with improved fabrication tolerance. The inter-modal XT performance of the HMPSA is characterized by transmitting an optical signal from a defined input port and then measuring the transmission spectrum at all output ports sequentially. All MZI heating powers are manually adjusted to enable maximum output at the same port. For example, when we measure the inter-modal XT from port I₁-TE₀ to port O₂-TE₁, the MZI switches for the

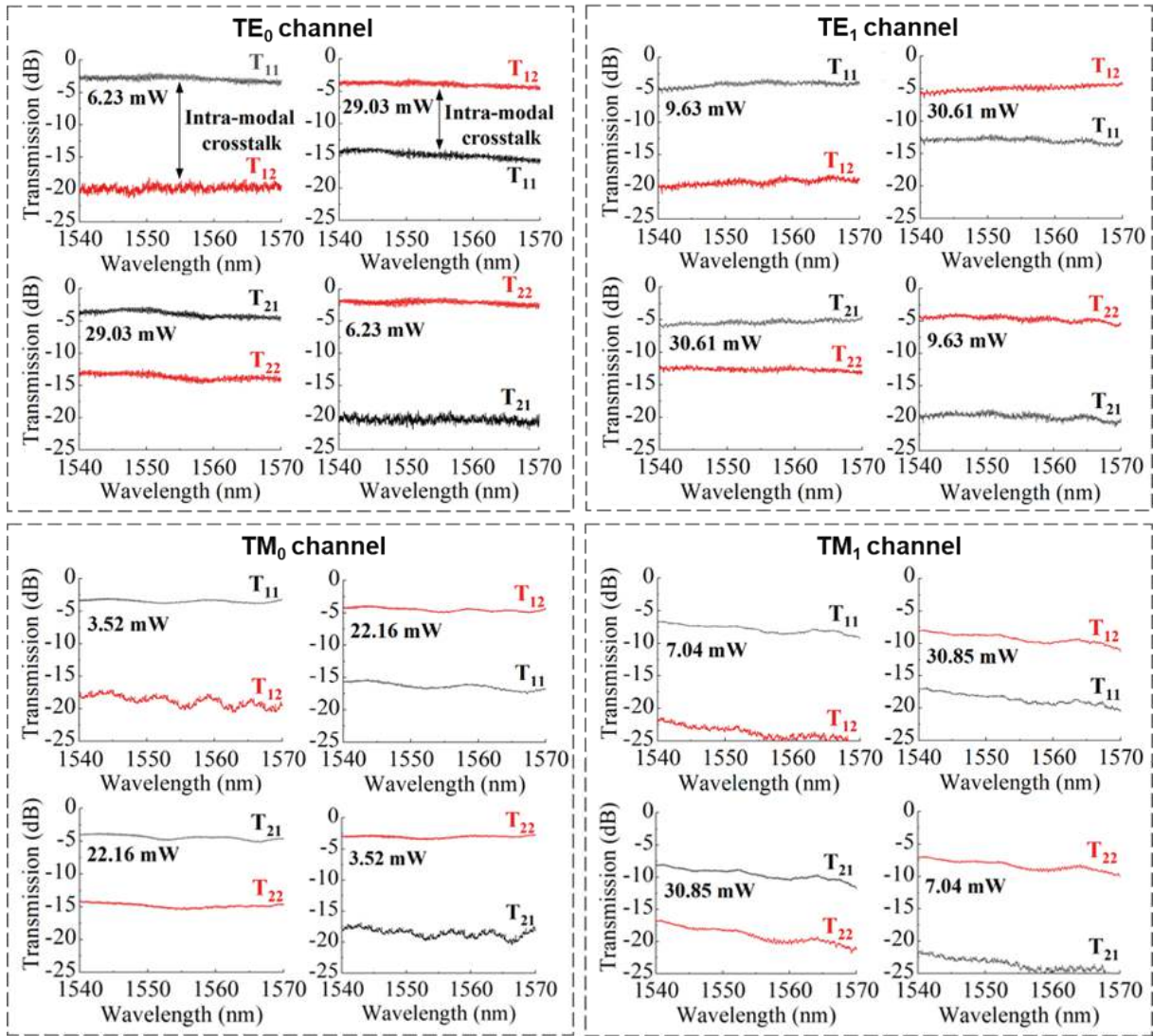


Fig. 4. (Color online) Results of measured intra-modal crosstalk.

port I_1 -TE₀ and I_1 -TE₁ are both set to output at the port O_2 . As shown in Fig. 3, the measured inter-modal XT values of the fabricated device are lower than -15.86 dB at 1550 nm for all the channels.

Fig. 4 shows the measured intra-modal XT introduced by the high-speed MZI switches. For the port I_1 -TE₀, the measured intra-modal XT are below -10.13 dB at 1550 nm. For all the inputs, the overall intra-modal XT are lower than -7.32 dB at 1550 nm. The relatively large crosstalk introduces significant, but tolerable, impairments for a quadrature phase-shift keying (QPSK) format by using an on-chip self-homodyne coherent detection scheme^[28]. Further intra-modal XT reduction can be realized via two MZI switches^[29] or using the variable coupler^[30].

We then measure the dynamic routing performance of the switch by applying a 1 MHz square-wave voltage signal to the device. The peak-to-peak drive voltage is 1.1 V biased at a direct current voltage at 0.8 V. Fig. 5 shows the measured response for the switch. The measured 10%–90% switching time upon electrical tuning are 11 and 10 ns for the rising and falling edges, respectively.

4. Conclusion

In conclusion, a 2×2 HMPA is experimentally demon-

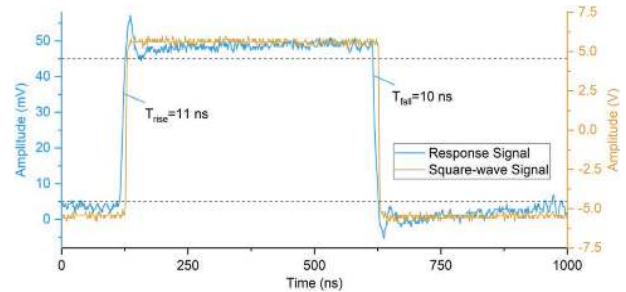


Fig. 5. (Color online) Measured dynamic response of the switch. Yellow and blue curves represent the applied square-wave voltage signal and measured signal dynamic switching, respectively. The dotted lines donate the 10% and 90% of the peak voltage.

strated based on EO MZIs. The ILs of the switch are 3.55–9.03 dB at 1550 nm. The measured inter-modal and intra-modal XT values are better than -15.86 and -7.32 dB at 1550 nm, respectively. The switching time (10%–90%) for the rising and falling edges are 11 and 10 ns, respectively. The demonstrated silicon 2×2 HMPA has promising potential for future high-speed optical networks with switching time of only nanoseconds. Furthermore, this scheme can be extended to higher-order modes by employing cascaded subwavelength-grating-based directional couplers^[31].

Acknowledgements

This work was supported in part by the National Key Research and Development Program of China under Grant 2019YFB2203600, the National Natural Science Foundation of China (NSFC) under Grant 61975115/61835008/62035016, and the Science and Technology Commission of Shanghai Municipality under Grant 2017SHZDZX03.

References

- [1] Winzer P J, Neilson D T, Chraplyvy A R. Fiber-optic transmission and networking: The previous 20 and the next 20 years. *Opt Express*, 2018, 26, 24190
- [2] Stern B, Zhu X L, Chen C P, et al. On-chip mode-division multiplexing switch. *Optica*, 2015, 2, 530
- [3] Xiong Y L, Priti R B, Liboiron-Ladouceur O. High-speed two-mode switch for mode-division multiplexing optical networks. *Optica*, 2017, 4, 1098
- [4] Yao Y H, Cheng Z, Dong J J, et al. Performance of integrated optical switches based on 2D materials and beyond. *Front Optoelectron*, 2020, 13, 129
- [5] Zhao Y H, Wang X, Gao D S, et al. On-chip programmable pulse processor employing cascaded MZI-MRR structure. *Front Optoelectron*, 2019, 12, 148
- [6] Su Y K, Zhang Y, Qiu C Y, et al. Silicon photonic platform for passive waveguide devices: Materials, fabrication, and applications. *Adv Mater Technol*, 2020, 5, 1901153
- [7] Luo L W, Ophir N, Chen C P, et al. WDM-compatible mode-division multiplexing on a silicon chip. *Nat Commun*, 2014, 5, 3069
- [8] Jia H, Yang S L, Zhou T, et al. WDM-compatible multimode optical switching system-on-chip. *Nanophotonics*, 2019, 8, 889
- [9] Han L S, Kuo B P P, Alic N, et al. Silicon Photonic Wavelength and Mode Selective Switch for WDM-MDM networks. 2019 Optical Fiber Communication Conference (OFC), 2019, 1
- [10] Jia H, Zhou T, Zhang L, et al. Optical switch compatible with wavelength division multiplexing and mode division multiplexing for photonic networks-on-chip. *Opt Express*, 2017, 25, 20698
- [11] Zhang Y, He Y, Zhu Q M, et al. On-chip silicon photonic 2×2 mode- and polarization-selective switch with low inter-modal crosstalk. *Photon Res*, 2017, 5, 521
- [12] Zhang Y, Zhang R H, Zhu Q M, et al. Architecture and devices for silicon photonic switching in wavelength, polarization and mode. *J Light Technol*, 2019, 38, 215
- [13] Dai D, Wang J, Shi Y. Silicon mode (de)multiplexer enabling high capacity photonic networks-on-chip with a single-wavelength-carrier light. *Opt Lett*, 2013, 38, 1422
- [14] Liu Y Y, Shainline J M, Zeng X G, et al. Ultra-low-loss CMOS-compatible waveguide crossing arrays based on multimode Bloch waves and imaginary coupling. *Opt Lett*, 2014, 39, 335
- [15] Siew S Y, Li B, Gao F, et al. Review of silicon photonics technology and platform development. *J Light Technol*, 2021, 39, 4374
- [16] Driscoll J B, Grote R R, Souhan B, et al. Asymmetric Y junctions in silicon waveguides for on-chip mode-division multiplexing. *Opt Lett*, 2013, 38, 1854
- [17] Chen W, Wang P, Yang J. Mode multi/demultiplexer based on cascaded asymmetric Y-junctions. *Opt Express*, 2013, 21, 25113
- [18] Uematsu T, Ishizaka Y, Kawaguchi Y, et al. Design of a compact two-mode multi/demultiplexer consisting of multimode interference waveguides and a wavelength-insensitive phase shifter for mode-division multiplexing transmission. *J Light Technol*, 2012, 30, 2421
- [19] Sun Y, Xiong Y L, Ye W N. Experimental demonstration of a two-mode (de)multiplexer based on a taper-etched directional coupler. *Opt Lett*, 2016, 41, 3743
- [20] Jia H, Zhang L, Ding J, et al. Microring modulator matrix integrated with mode multiplexer and de-multiplexer for on-chip optical interconnect. *Opt Express*, 2017, 25, 422
- [21] Dai D, Mao M. Mode converter based on an inverse taper for multimode silicon nanophotonic integrated circuits. *Opt Express*, 2015, 23, 28376
- [22] Jiang W F, Miao J Y, Li T. Compact silicon 10-mode multi/demultiplexer for hybrid mode- and polarisation-division multiplexing system. *Sci Rep*, 2019, 9, 13223
- [23] Zhang Y, He Y, Wang H W, et al. Ultra-broadband mode size converter using on-chip metamaterial-based Luneburg lens. *ACS Photonics*, 2021, 8, 202
- [24] Zheng X, Chang E, Amberg P, et al. A high-speed, tunable silicon photonic ring modulator integrated with ultra-efficient active wavelength control. *Opt Express*, 2014, 22, 12628
- [25] Jayatilaka H, Murray K, Guillén-Torres M Á, et al. Wavelength tuning and stabilization of microring-based filters using silicon in-resonator photoconductive heaters. *Opt Express*, 2015, 23, 25084
- [26] Dai D X, Li C L, Wang S P, et al. 10-channel mode (de)multiplexer with dual polarizations. *Laser Photonics Rev*, 2018, 12, 1700109
- [27] Xu D X, Schmid J H, Reed G T, et al. Silicon photonic integration platform — have we found the sweet spot. *IEEE J Sel Top Quantum Electron*, 2014, 20, 189
- [28] Huang H Z, Huang Y T, He Y, et al. Demonstration of terabit coherent on-chip optical interconnects employing mode-division multiplexing. *Opt Lett*, 2021, 46, 2292
- [29] Okuno M, Kato K, Nagase R, et al. Silica-based 8×8 optical matrix switch integrating new switching units with large fabrication tolerance. *J Light Technol*, 1999, 17, 771
- [30] Suzuki K, Cong G, Tanizawa K, et al. Ultra-high-extinction-ratio 2×2 silicon optical switch with variable splitter. *Opt Express*, 2015, 23, 9086
- [31] He Y, Zhang Y, Zhu Q M, et al. Silicon high-order mode (de)multiplexer on single polarization. *J Light Technol*, 2018, 36, 5746



Yihang Dong got his BS from Shanghai University in 2020. Then he joined the State Key Laboratory of Advanced Optical Communication Systems and Networks with the guide of Professor Zhang for relative research.



Yong Zhang received his PhD degree from the Huazhong University of Science and Technology, Wuhan, China. He joined Shanghai Jiao Tong University, Shanghai, China, as an assistant professor in 2015 and became an associate professor in 2019. His research areas cover silicon photonics devices, polarization, and mode devices.



Yikai Su received his PhD degree in electrical engineering from Northwestern University, Evanston, IL, USA in 2001. He worked at Crawford Hill Laboratory of Bell Laboratories and then joined the Shanghai Jiao Tong University as a full professor in 2004. His research areas cover silicon photonic devices for information transmission and switching.